frontiers in Neurology

ORIGINAL RESEARCH
published: 05 June 2019
doi: 10.3389/fneur.2019.00587

Modulation of Resting Connectivity Between the Mesial Frontal Cortex and Basal Ganglia

*Traian Popa[1†], Laurel S. Morris[2,3†], Rachel Hunt[1,4], Zhi-De Deng[5,6], Silvina Horovitz[1], Karin Mente[1], Hitoshi Shitara[1], Kwangyeol Baek[7], Mark Hallett[1] and Valerie Voon[2,7]**

[1] Human Motor Control Section, Medical Neurology Branch, National Institute of Neurological Disorders and Stroke, National Institutes of Health, Bethesda, MD, United States, [2] Behavioural and Clinical Neuroscience Institute, University of Cambridge, Cambridge, United Kingdom, [3] Department of Psychology, University of Cambridge, Cambridge, United Kingdom, [4] Oakland University William Beaumont School of Medicine, Rochester, MI, United States, [5] Non-Invasive Neuromodulation Unit, Experimental Therapeutics & Pathophysiology Branch, National Institute of Mental Health, National Institutes of Health, Bethesda, MD, United States, [6] Department of Psychiatry and Behavioral Sciences, Duke University School of Medicine, Durham, NC, United States, [7] Department of Psychiatry, University of Cambridge, Cambridge, United Kingdom

OPEN ACCESS

Edited by:
Matteo Bologna,
Sapienza University of Rome, Italy

Reviewed by:
Alessandro Tessitore,
Università Degli Studi Della Campania Luigi Vanvitelli Caserta, Italy
Ying-Zu Huang,
Chang Gung University, Taiwan

***Correspondence:**
Valerie Voon
vv247@cam.ac.uk

†These authors have contributed equally to this work

Specialty section:
This article was submitted to Movement Disorders, a section of the journal Frontiers in Neurology

Received: *18 February 2019*
Accepted: *17 May 2019*
Published: *05 June 2019*

Citation:
Popa T, Morris LS, Hunt R, Deng Z-D, Horovitz S, Mente K, Shitara H, Baek K, Hallett M and Voon V (2019) Modulation of Resting Connectivity Between the Mesial Frontal Cortex and Basal Ganglia. Front. Neurol. 10:587. doi: 10.3389/fneur.2019.00587

Background: The mesial prefrontal cortex, cingulate cortex, and the ventral striatum are key nodes of the human mesial fronto-striatal circuit involved in decision-making and executive function and pathological disorders. Here we ask whether deep wide-field repetitive transcranial magnetic stimulation (rTMS) targeting the mesial prefrontal cortex (MPFC) influences resting state functional connectivity.

Methods: In Study 1, we examined functional connectivity using resting state multi-echo and independent components analysis in 154 healthy subjects to characterize default connectivity in the MPFC and mid-cingulate cortex (MCC). In Study 2, we used inhibitory, 1 Hz deep rTMS with the H7-coil targeting MPFC and dorsal anterior cingulate (dACC) in a separate group of 20 healthy volunteers and examined pre- and post-TMS functional connectivity using seed-based and independent components analysis.

Results: In Study 1, we show that MPFC and MCC have distinct patterns of functional connectivity with MPFC–ventral striatum showing negative, whereas MCC–ventral striatum showing positive functional connectivity. Low-frequency rTMS decreased functional connectivity of MPFC and dACC with the ventral striatum. We further showed enhanced connectivity between MCC and ventral striatum.

Conclusions: These findings emphasize how deep inhibitory rTMS using the H7-coil can influence underlying network functional connectivity by decreasing connectivity of the targeted MPFC regions, thus potentially enhancing response inhibition and decreasing drug-cue reactivity processes relevant to addictions. The unexpected finding of enhanced default connectivity between MCC and ventral striatum may be related to the decreased influence and connectivity between the MPFC and MCC. These findings are highly relevant to the treatment of disorders relying on the mesio-prefrontal-cingulo-striatal circuit.

Keywords: cingulate cortex, ventral striatum, mesial prefrontal cortex, transcranial magnetic stimulation, resting state connectivity

INTRODUCTION

Neuromodulation with magnetic stimulation is emerging as a valuable treatment alternative for a wide range of psychiatric and neurologic disorders (1). Repetitive transcranial magnetic stimulation (rTMS) is a technique that can be used to apply multiple brief magnetic pulses to neuronal structures, thus transiently modulating neural excitability in a manner that is dependent mainly on the intensity and frequency of stimulation (2). It is a non-invasive, non-pharmacological, and safe treatment, in which abnormal communication within neuronal networks can be entrained and modified. Depending on the target, the depth at which stimulation occurs appears to be a crucial factor underlying potential therapeutic efficacy in certain disorders, such as major depressive disorder (3–5). In this study, we investigate the modulation of resting neural activity in mesial prefrontal-striatal circuits in healthy subjects by inhibitory deep wide-field stimulation with an Hesed (H-)7 coil (6, 7).

Fronto-striatal circuits are critical for the processing of reward, anticipation of outcomes, and behavioral control (8–11). Latent neural network organization and behavioral mechanisms in humans can be explored with resting state functional magnetic resonance imaging (fMRI) connectivity (rsFC), a method that measures the synchronization between intrinsic low-frequency fluctuations of brain regions in the absence of any specific task (12–14). Since the connections identified at rest closely mirror anatomical connections (15) and predict brain activations associated with behavioral performance (16), rsFC is an important tool for characterizing *in vivo* circuit-level dynamics, which may support particular behavioral responses (17, 18).

Studies of substance use disorders have revealed the critical role of fronto-striatal circuits, highlighting large scale disruptions in functional connectivity between the mesolimbic reward system and cortical regions involved in decision making and executive function (e.g., ventromedial prefrontal cortex, dorsolateral prefrontal cortex)(19–27). In particular, altered rsFC between the dorsal and ventral mesial prefrontal cortex (d/vMPFC), anterior cingulate cortex (ACC) and ventral striatum (VS) is most consistently observed across disorders of addiction such as cocaine (28), heroin (29), nicotine (30–33), and even internet addiction (32–35), but also in obsessive-compulsive disorder (OCD) (34). Furthermore, vMPFC activity seems to be tightly linked to dMPFC activity (36, 37). Thus, understanding whether and how deep rTMS targeting the MPFC influences the connected networks is critical to its potential clinical efficacy.

In Study 1, we first assess rsFC between MPFC and striatum in a relatively large sample of healthy controls. In Study 2, we then ask whether inhibitory deep wide-field stimulation with an H7-coil positioned over the MPFC [which, given the non-focal nature of the H7-coil (38, 39), we have defined here as supplementary motor area (SMA), preSMA, and dMPFC] influences rsFC with VS in a separate group of healthy controls. We focused on VS given its aberrant rsFC observed in pathological disorders as well as in our findings in Study 1 of negative connectivity of MPFC with VS and positive connectivity of mid-cingulate with VS. We hypothesize that low-frequency inhibitory rTMS will decrease rsFC of the MPFC with VS.

METHODS AND MATERIALS

Protocol Design and Participants

In Study 1, seed to whole brain intrinsic rsFC was examined for the mesial PFC (SMA, pre-SMA and dMPFC) and the mid-cingulate. For intrinsic baseline mapping, blood-oxygenation level dependent (BOLD) fMRI data was collected during rest (10 min, eyes open, watching white fixation cross on black screen) from 154 healthy volunteers (71 females; age 31 ± 13 years) at the Wolfson Brain Imaging Center, University of Cambridge, UK, with a Siemens Tim Trio 3T scanner and 32-channel head coil.

In Study 2, we used inhibitory, 1 Hz rTMS deep wide-field stimulation with an H7-coil targeting the mesial PFC. In order to examine the effects of rTMS on neural fluctuations, we used both ROI-to-ROI analyses and confirmed findings with independent component analysis (ICA). Resting state fMRI data (10 min, eyes open, watching white fixation cross) was collected immediately before and after rTMS (average time between rTMS end and EPI sequence was 285 ± 27 s) in a separate group of 20 healthy volunteers (15 females; age 36 ± 12 years) at the National Institutes of Health (Bethesda, MD, USA) core fMRI Facility, with a Siemens Skyra 3T scanner and 32-channel head coil.

All subjects provided informed written consent. This study was approved by the Research Ethics Committee of the University of Cambridge and the Institutional Review Board of the National Institutes of Health.

Transcranial Magnetic Stimulation With the H-coil (Study 2)

To modulate the excitability of deep frontal areas in Study 2, we used a Hesed coil type 7 (H7-coil). Its design aims at stimulating frontal brain regions (i.e., the PFC) and reaching deep brain regions without increasing the electric field levels in the more superficial cortical regions (6, 40). Deep TMS using other coils (e.g., classical double-cone coil) can be uncomfortable due to excessive stimulation of superficial structures and painful muscular contractions. The frames of the inner rim of H7-coil are also flexible to accommodate a variety of human skull shapes and allow a comfortable and closer fit of the coils to the scalp (**Supplementary Figure S1**).

We first found the hotspot and determined the active motor threshold (AMT) of the *Tibialis anterior muscle*, as an area situated medially at a depth similar to our regions of interest (**Figure 1A**). The AMT was defined as the lowest intensity able to evoke a motor potential with an amplitude at least 200 μV above the background EMG activity of a 10% maximal voluntary contraction of the left Tibialis anterior in 5 out of 10 consecutive trials. The coil was always maintained in the midline to avoid the problem of left-right anatomical and functional asymmetry, on top of the unknown exact geometrical location of the maximum field intensity of the H7-coil. In this way, the threshold determined for the left TA corresponded to an intensity strong enough to evoke action potentials in the pyramidal neurons on the mesial cortex at that depth in each individual. Repetitive

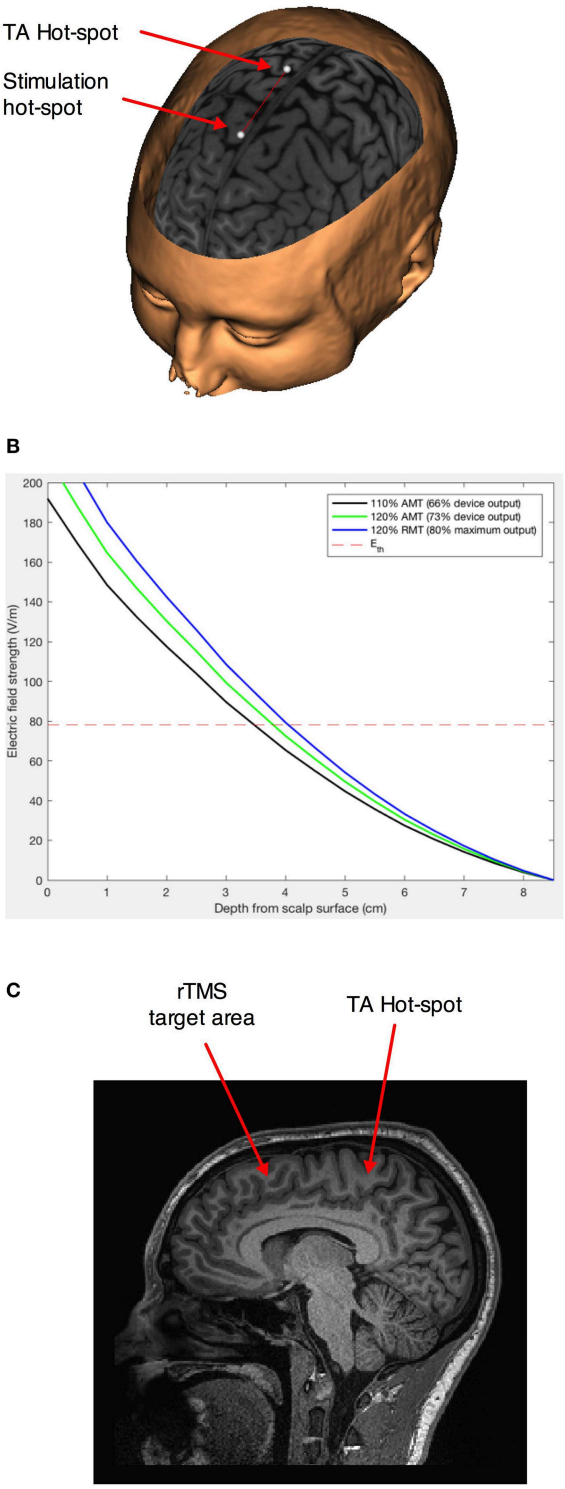

FIGURE 1 | Stimulation paradigm. **(A)** Schematic representation of the movement of the projection of the geometric center of the H7 coil 5 cm in front of the empirically found hot-spot for the left *Tibialis anterior* muscle (41, 42). The points represent an ideal (not neuronavigated) center of the interior of the H7 helmet. **(B)** Estimation of the induced electrical field intensity with distance from the coil for stimulation at 110% of the active motor threshold (AMT)—our *(Continued)*

FIGURE 1 | intensity of choice, and 120% AMT and 110% resting motor threshold—higher intensities distribution modeled for comparison. The dotted line represents the theoretical intensity of the induced electrical field for AMT. **(C)** Sagittal section showing the area in the dorso-mesial prefrontal cortex found at an equivalent depth to the *Tibialis anterior* motor representation.

TMS was delivered with a biphasic magnetic stimulator (Magstim Rapid2; The Magstim Company, Whitland, South West Wales, UK) with a frequency of 1 Hz and at 110% AMT intensity. Nine hundred pulses were administered over the MPFC, 5 cm anterior to the Tibialis anterior hot-spot, for 15 min. By choosing this location, we assured that the maximum field would cross areas BA 8/9, which are located in front of the peSMA (41, 42). When administered in accordance with current international guidelines, transcranial magnetic stimulation has been shown to be safe (43, 44), with few mild adverse effects, although we acknowledge that these safety guidelines are derived primarily from studies using conventional figure-8 coils.

We used medium intensity stimulation (i.e., 110% of the active motor threshold; average effective intensity 66 ± 8% of the maximum stimulator output) of the H7-coil, which would have penetrated effectively up to a depth of 3.5 cm from the surface of the scalp (**Figure 1B**), corresponding to the mesial PFC region (**Figure 1C**).

Resting State Functional MRI

The following describes the resting state acquisitions and analyses used for Study 1 and 2.

Acquisition Study 1: Functional images were acquired with a multi-echo echo planar imaging sequence with online reconstruction (repetition time (TR), 2.47 s; flip angle, 78°; matrix size 64 × 64; resolution 3.0 × 3.0 × 3.0 mm; FOV, 240 mm; 32 oblique slices, alternating slice acquisition slice thickness 3.75 mm with 10% gap; iPAT factor, 3; bandwidth (BW) = 1,698 Hz/pixel; echo time (TE) = 12, 28, 44 and 60 ms).

Study 2: Functional images were acquired with a multi-echo echo planar imaging sequence (TR, 2.47s; flip angle, 70°; matrix size 70 × 60; in-plane resolution, 3.0 mm; FOV, 210 mm; 34 oblique slices, alternating slice acquisition slice thickness 3.0 mm with 0% gap; iPAT factor, 3; bandwidth (BW) = 2,552 Hz/pixel; TE = 12, 28, 44, and 60 ms).

For both studies, anatomical images were acquired using a T1-weighted magnetization prepared rapid gradient echo (MPRAGE) sequence (76 × 240 field of view (FOV); resolution 1.0 × 1.0 × 1.0 mm; inversion time, 1,100 ms).

Preprocessing

The following processing and analyses apply to both resting state fMRI data unless stated otherwise. To enhance signal-to-noise ratio, we used multi-echo EPI sequence and independent component analysis (ICA), which allows data to be denoised for motion, physiological, and scanner artifacts in a robust manner based on physical principles (45).

Multi-echo independent component analysis (ME-ICA v2.5 beta6; http://afni.nimh.nih.gov) was used for data analysis and denoising. ME-ICA decomposes the functional data into independent components using FastICA. BOLD percent signal changes are linearly dependent on echo time (TE), a characteristic of the T2* decay. TE dependence of BOLD signal is measured using the pseudo-F-statistic, Kappa, with components that scale strongly with TE having high Kappa scores (46). Non-BOLD components are TE independent and measured by the pseudo-F-statistic, Rho. Components are thus categorized as BOLD or non-BOLD based on their Kappa and Rho weightings, respectively. Non-BOLD components are removed by projection, robustly denoising data. Each individual's denoised echo planar images were coregistered to their MPRAGE and normalized to the Montreal Neurological Institute (MNI) template. Spatial smoothing of the functional data was performed with a Gaussian kernel (full width half-maximum = 6 mm).

Region of Interest (ROI)-Driven Analysis

We performed ROI-driven functional connectivity analysis using CONN-fMRI Functional Connectivity toolbox (47) for Statistical Parametric Mapping SPM8 (http://www.fil.ion.ucl.ac.uk/spm/software/spm8/), using denoised, coregistered, smoothed functional data. The time course for each voxel was temporally band-pass filtered ($0.008 < f < 0.09$ Hz). Each individual's anatomical scan was segmented into gray matter, white matter and cerebrospinal fluid. Significant principle components of the signals from white matter and cerebrospinal fluid were removed.

Study 1: Intrinsic functional connectivity mapping

For intrinsic rsFC mapping in 154 healthy volunteers, ROI-to-whole brain connectivity was computed for mesial PFC and mid cingulate ROI's. Connectivity maps were thresholded at FWE $p < 0.05$ whole brain corrected. Both positive and negative functional connectivity was examined across the whole brain. Anatomically-defined ROIs were manually created or altered using MarsBaR ROI toolbox (48) for SPM (see **Supplementary Methods** for seed definitions).

Study 2: Effects of rTMS: ROI-based

To address the *a priori* hypothesis, ROI-to-ROI functional connectivity was first computed using Pearson's correlation between BOLD time courses for mesial PFC with ventral striatum, both pre- and post-TMS. These were entered into a paired samples *t*-test to compare between pre- and post-TMS. For the *a priori* ROI-to-ROI functional connectivity analysis between the mesial PFC and VS, $p<0.05$ was considered significant. On an exploratory basis, to assess the impact of rTMS on rsFC of deeper structures such as the mid-cingulate which lies immediately below the mesial PFC, ROI-to-ROI functional connectivity of mesial PFC to mid cingulate and mid cingulate to VS were examined pre- and post-TMS. $P<0.025$ was considered significant (Bonferonni corrected for multiple comparisons). The VS anatomical ROI has previously been used (49) and hand drawn using MRIcro (http://www.cabiatl.com/mricro/mricro/) based on a published definition of VS (50).

Effects of rTMS: Independent Component Analysis (Study 2)

To confirm the ROI-to-ROI findings, we then conducted ICA. While ICA has been shown to engender statistically similar results as seed based approaches in healthy volunteers (51), ICA is a multivariate data-driven approach that requires fewer *a priori* assumptions and takes into account interacting networks. Therefore, if TMS affects larger scale neural networks, ICA should succeed in highlighting this. Denoised, coregistered, and smoothed functional data was entered into ICA analysis using FSL MELODIC 3.14 software (FMRIB, University of Oxford, UK; www.fmrib.ox.ac.uk/fsl/melodic2/index.html) that performs probabilistic ICA to decompose data into independently distributed spatial maps and associated time courses to identify independent component variables (52). A high model order of 40 was used as a fair compromise between under- and over-fitting (53). Multi-session temporal concatenation was used to allow computation of unique temporal responses per subject/session. Comparisons between pre- and post-TMS was performed using FSL dual regression for reliable and robust (54) voxel-wise comparisons using non-parametric permutation testing with 5,000 permutations and using threshold free cluster enhancement (TFCE) controlling for multiple comparisons (55). Group differences of components that include MPFC were calculated with $p < 0.05$ thresholds.

RESULTS

Baseline Mapping

Intrinsic resting state whole brain connectivity maps for mesial PFC and mid cingulate are displayed in **Figure 2** and reported in **Supplementary Tables S1, S2**. Both positive and negative functional connectivity are displayed. Mesial PFC and mid cingulate showed opposite patterns of connectivity with ventral striatum: mesial PFC had negative but mid cingulate had positive functional connectivity with VS.

Effects of TMS

Focusing on our *a priori* hypothesis, we show that after rTMS, mesial PFC had reduced functional connectivity with ventral striatum ($t = 2.201$, $p = 0.043$) (**Figure 3**). We then show an effect on mid-cingulate functional connectivity with reduced functional connectivity following rTMS between the mesial PFC and mid-cingulate ($t = 4.325$, $p = 0.001$) and enhanced functional connectivity between mid-cingulate and VS ($t = -2.495$ $p = 0.024$).

We conducted ICA on the resting state data pre- and post-rTMS to confirm our *a priori* hypothesis and analysis. Out of 40 components, three included prominent mesial frontal cortex (**Figure 4**). Of the three mesial frontal network components, dual regression revealed that one of these components (IC11) was significantly decreased post-rTMS (TFCE $p = 0.0360$). The IC00 included prominent dmPFC; the IC11 included dmPFC, preSMA, and SMA; the IC38 included prominent anterior and mid cingulate, and dmPFC. The dmPFC/ACC can be considered part of the dorsal attention network.

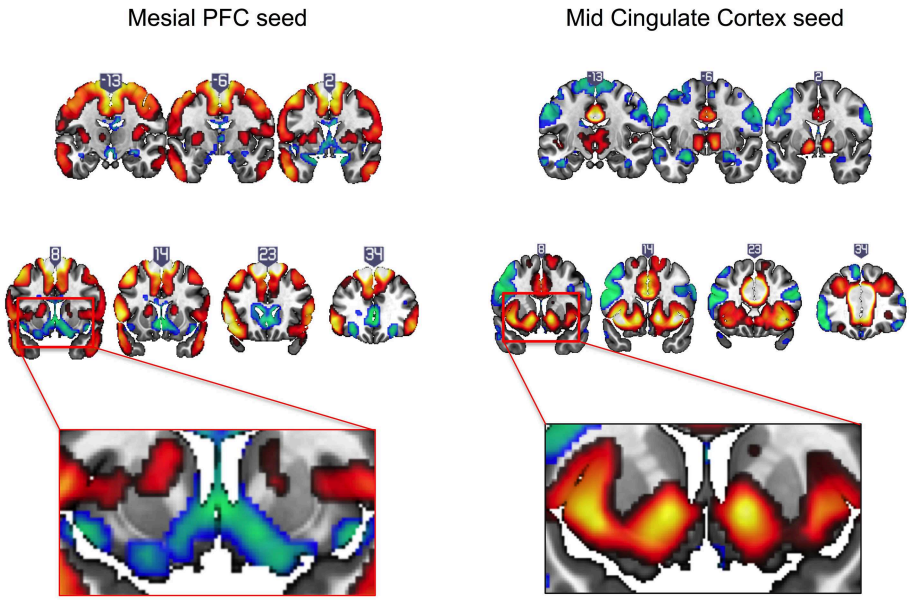

FIGURE 2 | Intrinsic resting state connectivity maps for mesial prefrontal cortex (PFC) and mid cingulate cortex seeds to whole brain in healthy controls. Positive (yellow-red) and negative (green-blue) functional connectivity are displayed. The rectangular insets at y = 8 highlighting differences in direction of connectivity of the striatum are shown for the mesial PFC (bottom row, left) and mid cingulate (bottom row, right). Coronal images (y-values shown above image) are thresholded at whole brain family-wise error, corrected $p < 0.05$ on a standard MNI template.

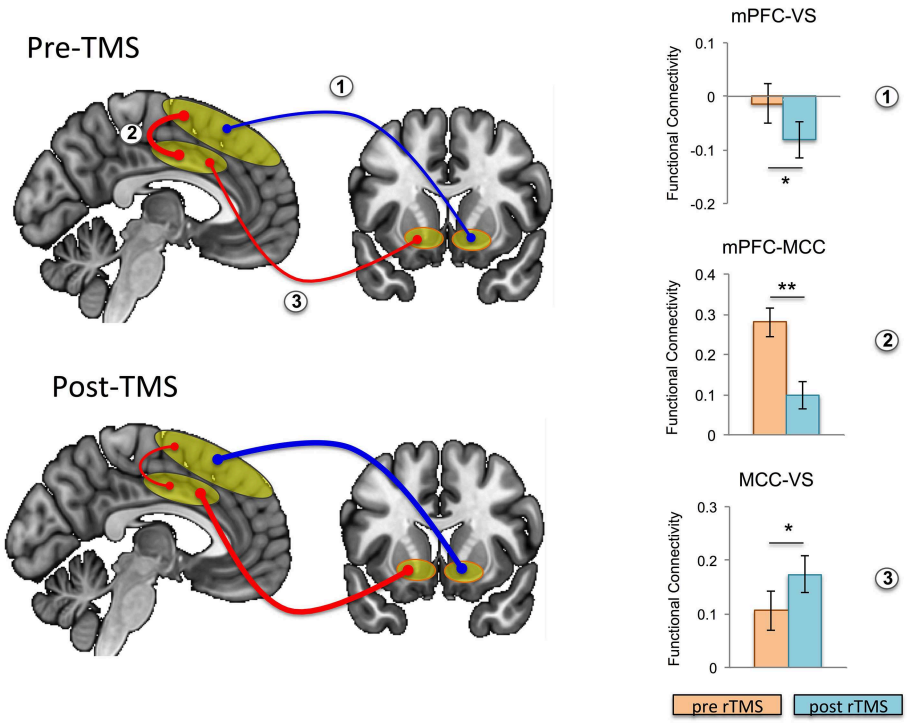

FIGURE 3 | Effects of repetitive transcranial magnetic stimulation (rTMS) on intrinsic functional connectivity in healthy controls. Functional connectivity is schematically illustrated at baseline (i.e., pre-rTMS; top left) and post-rTMS (bottom left); pre- and post-rTMS effects on seed-to-seed functional connectivity are shown in the bar graphs. After rTMS, functional connectivity between mesial prefrontal cortex (mPFC) and ventral striatum (VS), and between mPFC and mid cingulate cortex (MCC) was reduced, while functional connectivity between MCC and VS was increased (the thickness of the arrows correspond to strength, and color to direction: red, positive connectivity; blue, negative connectivity). Error bars are shown as standard error of the mean. *$p < 0.05$, **$p = 0.001$.

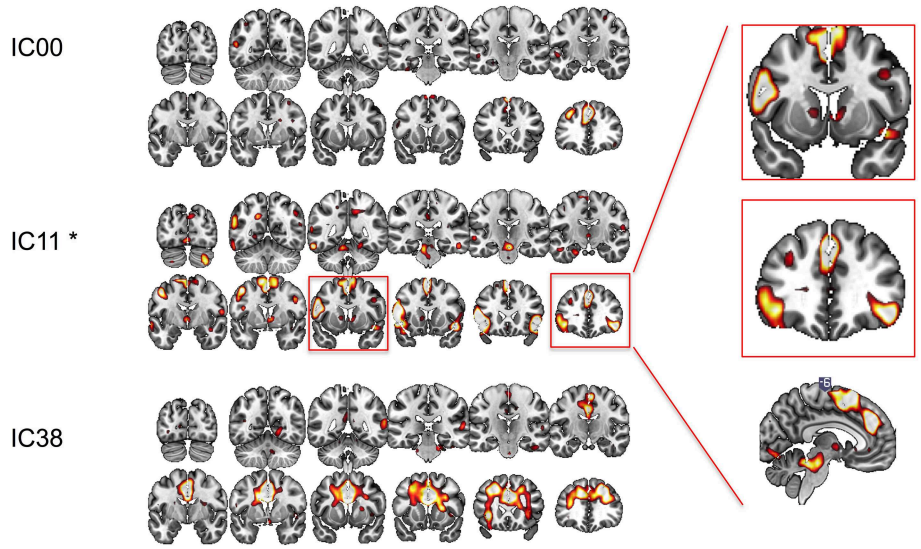

FIGURE 4 | Functional connectivity at rest between different regions of interest explored with independent component analysis pre- and post-rTMS. Three components included prominent mesial-frontal cortex (IC00, IC11, and IC38). The insert shows IC11, which included supplementary motor area (SMA), pre-SMA, dorsomedial prefrontal cortex/dorsal cingulate, and ventral caudate/striatum, and bilateral inferior frontal cortices was significantly decreased post-rTMS. *$p < 0.05$.

DISCUSSION

We characterized the effects of deep wide-field mesial prefrontal rTMS on the resting-state functional network in healthy individuals. We first mapped intrinsic functional connectivity of mesial prefrontal and mid-cingulate cortical regions in a large sample of healthy volunteers. We found that intrinsic functional connectivity of the mesial PFC region of interest with ventral striatum was negative, whereas the intrinsic functional connectivity of mid-cingulate connectivity with ventral striatum was positive. Then, we show that deep wide-field inhibitory rTMS targeting the mesial PFC decreases rsFC between this broad mesial PFC region and the ventral striatum. These findings were further confirmed with ICA analysis, a data-driven approach. Based on the modeling of the magnetic field distribution, induced-electrical field decay, and the depth of the target region stimulated, we likely also inhibited directly the dorsal posterior regions of Brodmann Area 32, corresponding to dorsal anterior cingulate—a fact subsequently confirmed by the ICA analysis. Inhibitory rTMS also decreased functional connectivity of the "stopping" network including pre-SMA, right inferior frontal cortex, and ventral caudate. This is in line with previous reports, in which inhibitory rTMS (including continuous theta burst stimulation) targeting the pre-SMA with standard figure-of-eight coil has been shown to enhance motor response inhibition (56).

We also found effects of deep rTMS on connectivity between deeper structures such as the mid-cingulate cortex, which was unlikely to be directly stimulated with our stimulation parameters: decreased rsFC between the broad mesial PFC and mid-cingulate cortex, and, unexpectedly, enhanced rsFC between mid-cingulate cortex and ventral striatum. These findings suggest that while deep wide-field mesial prefrontal inhibitory rTMS might directly decrease the functional connectivity between the stimulated and the connected structures, the decreased influence from superficial cortical regions might indirectly enhance the intrinsic connectivity between remote structures (i.e., the mid-cingulate cortex and ventral striatum).

Application of rTMS to superficial cortical regions with the strongest negative functional connectivity with subgenual ACC has already been shown to be most clinically efficacious in reducing depression (57). Thus, based on the deep cortical or subcortical structure of interest for a given disorder, appropriate superficial sites for rTMS can be selected based on intrinsic functional connectivity strengths and patterns. Since we demonstrate in our second study that there is an exaggeration of intrinsic functional connectivity strengths with deep inhibitory rTMS, detailed mapping of baseline connectivity patterns will inform the selection of rTMS targets with the aim to "normalize" aberrant underlying functional connectivity in disease states. The outcome of this modulation could be of interest in the treatment of disorders relying on the mesioprefrontal-cingulo-striatal circuit.

The H-coil series was originally designed to have a significant impact on deep structures, like the anterior cingulate cortex (6, 7). It has been used with different degrees of success to treat depression (58, 59), alcohol use disorders (60), nicotine addiction (61), and even as adjunctive therapy in Parkinson's disease (62), blepharospasm (63), and chronic migraine (64). Due to the quick drop in TMS efficacy with increasing target depth (65), it has been proposed that any stimulation outside the primary motor cortex should be referenced to motor cortex excitability and adjusted to the target depth (66, 67). The original assertion that the H-coil can modulate the activity of deep structures has been based mainly on calculating the intensity of the induced electrical

field at different depths for a given stimulation intensity (40). However, other factors can significantly influence the efficacy of rTMS, including the orientation of the coil (68–70) and the configuration of the subjacent and/or target cortex (71–75), as well as the secondary electrical fields generated at the boundary between the cerebrospinal fluid and the gray matter (76). Subsequent studies of the distribution of the magnetic field generated by the H-coil revealed that the largest field intensity variation and hence, the functional effect covers first the mesial neuronal structures in close proximity to the coil, i.e., superior MF areas, like dMPFC, pre-SMA, SMA (40, 77–79), and only secondarily deeper structures such as the cingulate cortex if stimulation intensity is high enough (7, 40). In order to reach the stimulation threshold of neurons, a total field of 30–100 V/m is needed, depending on the neurons (80). Since focal coils, like flat 8-shaped or double-cone coils, produce very strong fields that decay fast as a function of distance, 500 V/m would be induced at 1 cm depth (i.e., scalp) for 50 V/m at 5 cm, which would be very uncomfortable due to superficial muscle contraction under the stimulated site (6). According to our simulations (**Figure 1B**) using a spherical head model, the structure of the H7-coil induces only 150 V/m at 1 cm in the same conditions, albeit at the cost of focality, making it more tolerable. In this study, we used medium intensity stimulation (i.e., 110% of the active motor threshold; average effective intensity 66 ± 8% of the maximum stimulator output), which would have stimulated a region of interest corresponding to the mesial PFC. This allowed us to influence directly the output of these areas and indirectly the activity of functionally linked structures (81–86). Based on the simulated model of the target and depth reached using our stimulation parameters, we likely directly stimulated down to dorsal posterior regions of Brodmann Area 32 corresponding to dorsal anterior cingulate. However, it is unlikely that we directly stimulated the mid-cingulate; thus any change in connectivity observed in the mid-cingulate would likely be an indirect effect via changing the functional output of connected areas. Here, we extend the understanding of the effects of magnetic stimulation over the middle frontal areas, following previous TMS studies investigating more superficial stimulation of the lateral frontal areas (57, 87–89). Subsequent studies are indicated to investigate the influence of higher intensities and higher frequencies (90) on rsFC of frontal superficial and deep structures, when applied with coils designed to reach broader regions. The magnetic field generated by an H7-coil is covering a much wider area of the frontal lobe, but as with the classical double-cone coil, which has a similar shape but smaller, the magnetic field generated at the edges of the coil is assumed to be non-focal and weak enough as not to induce a meaningful neuronal depolarization.

We delivered magnetic pulses at 1 Hz for 15 min. This frequency can induce a long term depression (LTD)-like effect in the targeted neuronal networks that outlasts the stimulation for a sufficient duration to assess the influence on resting-state fMRI (91–94). By using low stimulation intensities, we effectively depressed the excitability of the superior mesial prefrontal areas and possibly also the dorsal posterior region of Brodmann Area 32 corresponding to dorsal anterior cingulate cortex. An LTD-like effect would thus decrease neuronal excitability in the mesial PFC, rendering it less responsive to incoming information. Decreased responsiveness would functionally decouple this region from both neighboring and deeper structures. Indeed, we found reduced functional connectivity of the broad mesial PFC with mid-cingulate, and between the broad mesial PFC and ventral striatum, with ICA confirming decreases in the network including mesial PFC, dorsal anterior cingulate and ventral caudate/ventral striatum. Since the fronto-striatal network relies on a dynamic equilibrium between its different parts (11, 95, 96), functionally "nudging" one part should entrain a reconfiguration of all functional connections, including functional connectivity between remote regions receiving projections from the stimulated region. This seems to be the case in our study: we found increased functional connectivity between the mid-cingulate area and ventral striatum after inhibiting the mesial PFC.

The outcome of this modulation could be of interest in treatment of disorders relying on the mesioprefrontal-cingulo-striatal circuit. In healthy humans, this circuit is involved in cognitive and emotional control, error and conflict monitoring (97–99), response inhibition (100), and positive and negative prediction error and anticipation (101–103). Abnormal cortico-ventro striatal hyperconnectivity has been OCD (104–106) and addictions [for a review see (107)]. In disorders of addiction, decreased functional connectivity between the ventral striatum and the cingulate cortex bilaterally is commonly observed (29, 32), with enhanced dorsal cingulate and ventral striatal activity in the context of drug cues (108). Numerous targets had been proposed for invasive deep brain stimulation aimed at correcting these imbalances, including the anterior limb of the internal capsule (109), subthalamic nucleus (110), and ventral striatum/nucleus accumbens (111). In order to avoid the risks of an invasive procedure, studies have explored stimulating other nodes of these networks that are accessible to TMS at the surface of the brain. Stimulation of the dorsolateral prefrontal cortex, is [arguably (58, 59)] successful in treatment-resistant major depressive disorder (4, 112), with modest results in OCD (113). On the other hand, stimulation of the dorso-medial prefrontal cortex (114) or preSMA/SMA complex (115–117) seems slightly more encouraging. Notably, there is no gold standard yet for the frequencies to be used. The stimulation frequencies used thus far in most studies cover a wide range including continuous delivery at 1 Hz, or intermittently at 10 or 18 Hz in 5 s trains separated by breaks of 10 s. While 1 Hz stimulation is known to induce LTD-like effects, the mechanism of action and the eventual outcome of other multiple medium-frequency trains is still open to debate and investigation (118, 119).

Wide inhibitory stimulation of the dorso-mesial areas of the frontal lobe might have both clinical and mechanistic benefit. Wider superficial stimulation has a clear clinical benefit allowing a reduction in the intensity of the stimulation with deeper stimulation, thus increasing patients' comfort and adherence by decreasing superficial muscle contraction, and minimizing risks. Aberrant activity in networks in psychiatric disorders may affect broader regions that can be targeted via wide inhibitory stimulation. We show that stimulation that is both wide and deep is associated with decreased connectivity between the mesial

prefrontal areas and deeper structures (like the mid-cingulate areas and ventral striatum), with possibly a secondary effect of increasing connectivity between cingulate and ventral striatum. Wider stimulation will also have a broader effect on multiple neural regions, impacting a wide range of cognitive functions. Using the H7-coil with inhibitory rTMS is thus consistent with both inhibition of the pre-SMA shown to enhance motor response inhibition (56) and decreased dorsal cingulate activity associated with drug cue reactivity (108). Therefore, the H7-coil has the capacity to both enhance the response inhibition associated with the stopping network in disorders of addiction, and decrease drug cue reactivity associated with the dorsal cingulate and ventral striatum. However, it is unclear whether decreasing dorsal cingulate activity across all conditions would be the optimal approach, as resting state functional connectivity between cingulate and ventral striatal regions are commonly decreased in disorders of addiction. Further studies investigating a state-specific effect of rTMS may be relevant with pairing H-coil stimulation with drug cues with or without concurrent response inhibition. It also remains to be established whether our findings are specific to wide-field deep rTMS or whether focal deep rTMS (which is be more difficult to tolerate) would show similar rsFC pattern changes within cingulate regions.

This study is not without limitations. While we did not have a sham control, we note that our findings revealed both increases and decreases in connectivity—suggesting that an order effect is unlikely to account for these observations. It is also technically impossible to achieve a realistic sham with the H-coil, since the real stimulation evokes a specific, unconfoundable small contraction of the anterior belly of the occipitofrontal muscle. The localization of the peak stimulus effect is also more difficult with the H-coil, since the coils' positions inside the helmet are flexible and the precise technical characteristics of the coils are proprietary to the company. We do present, however, an X-ray of the coil structure and the geometrical approximation of the coil used in the modeling of the magnetic field penetration depth **(Supplementary Figure S1)**. Subsequent studies testing higher frequencies and/or intensities are indicated, as well as repeated stimulation sessions (over minimum 4 weeks) in preparation for clinical trials.

We highlight that non-invasive wide and deep inhibitory brain stimulation appears to decrease the underlying functional connectivity of regions immediately within the stimulation zone while enhancing functional connectivity of deeper structures such as mid-cingulate to ventral striatum. This unexpected finding might be related to the decreased influence from superficial cortical regions via decreased cortico-cortical connectivity. A deep wide-field coil allows both greater tolerability and the capacity to influence multiple relevant neural regions and cognitive functions. These dissociable findings may be relevant particularly to disorders of addiction and OCD, and have implications for designing interventional deep rTMS studies.

DATA AVAILABILITY

The datasets generated for this study are available on request to the corresponding author.

ETHICS STATEMENT

This study was carried out in accordance with the recommendations of the Institutional Review Board (IRB) of the National Institutes of Health (NIH) with written informed consent from all subjects. All subjects gave written informed consent in accordance with the Declaration of Helsinki. The protocol was approved by the NIH IRB.

AUTHOR CONTRIBUTIONS

TP, LM, MH, and VV contributed conception and design of the study. TP, LM, RH, Z-DD, SH, and KM analyzed the data. LM and KB performed the statistical analysis. TP and LM wrote the first draft of the manuscript. Z-DD and SH wrote sections of the manuscript. All authors contributed to manuscript revision, read and approved the submitted version.

FUNDING

This study was supported in part by the Intramural Research Program of the National Institutes of Health, National Institute of Neurological Disorders and Stroke, and from VV Wellcome Trust Fellowship (093705/Z/10/Z).

ACKNOWLEDGMENTS

We thank our subjects for taking part in this study and the NMR Center personnel for the efficient assistance. This manuscript has been released as a Pre-Print (120) at https://www.biorxiv.org/content/10.1101/432609v1.

SUPPLEMENTARY MATERIAL

The Supplementary Material for this article can be found online at: https://www.frontiersin.org/articles/10.3389/fneur.2019.00587/full#supplementary-material

REFERENCES

1. Bersani FS, Minichino A, Enticott PG, Mazzarini L, Khan N, Antonacci G, et al. Deep transcranial magnetic stimulation as a treatment for psychiatric disorders: a comprehensive review. *Eur Psychiat.* (2013) 28:30–9. doi: 10.1016/j.eurpsy.2012.02.006
2. Roth Y, Padberg F, Zangen A. Transcranial magnetic stimulation of deep brain regions: principles and methods. In: Marcolin M, Padberg F, editors. *Transcranial Brain Stimulation for Treatment of Psychiatric Disorders*. Basel: Karger (2007). p. 204–24. doi: 10.1159/000101039
3. Berlim MT, McGirr A, Van den Eynde F, Fleck MP, Giacobbe P. Effectiveness and acceptability of deep brain stimulation (DBS) of the subgenual cingulate cortex for treatment-resistant depression: a systematic

review and exploratory meta-analysis. *J Aff Disord*. (2014) 159:31–8. doi: 10.1016/j.jad.2014.02.016
4. Berlim MT, Van den Eynde F, Tovar-Perdomo S, Chachamovich E, Zangen A, Turecki G. Augmenting antidepressants with deep transcranial magnetic stimulation (DTMS) in treatment-resistant major depression. *World J Biol Psychiatry*. (2014) 15:570–8. doi: 10.3109/15622975.2014.925141
5. Lefaucheur JP, Andre-Obadia N, Antal A, Ayache SS, Baeken C, Benninger DH, et al. Evidence-based guidelines on the therapeutic use of repetitive transcranial magnetic stimulation (rTMS). *Clin Neurophysiol*. (2014) 125:2150–206. doi: 10.1016/j.clinph.2014.05.021
6. Roth Y, Zangen A, Hallett M. A coil design for transcranial magnetic stimulation of deep brain regions. *J Clin Neurophysiol*. (2002) 19:361–70. doi: 10.1097/00004691-200208000-00008
7. Zangen A, Roth Y, Voller B, Hallett M. Transcranial magnetic stimulation of deep brain regions: evidence for efficacy of the H-coil. *Clin Neurophysiol*. (2005) 116:775–9. doi: 10.1016/j.clinph.2004.11.008
8. Miller EK. The prefrontal cortex and cognitive control. *Nat Rev Neurosci*. (2000) 1:59–65. doi: 10.1038/35036228
9. Hikosaka O, Isoda M. Switching from automatic to controlled behavior: cortico-basal ganglia mechanisms. *Trends Cogn. Sci*. (2010) 14:154–61. doi: 10.1016/j.tics.2010.01.006
10. Lee I, Lee CH. Contextual behavior and neural circuits. *Front Neural Circ*. (2013) 7:84. doi: 10.3389/fncir.2013.00084
11. Morris LS, Kundu P, Dowell N, Mechelmans DJ, Favre P, Irvine MA, et al. Fronto-striatal organization: defining functional and microstructural substrates of behavioural flexibility. *Cortex*. (2016) 74:118–33. doi: 10.1016/j.cortex.2015.11.004
12. Biswal B, Yetkin FZ, Haughton VM, Hyde JS. Functional connectivity in the motor cortex of resting human brain using echo-planar MRI. *Magn Res Med*. (1995) 34:537–41. doi: 10.1002/mrm.1910340409
13. Biswal BB, Van Kylen J, Hyde JS. Simultaneous assessment of flow and BOLD signals in resting-state functional connectivity maps. *NMR Biomed*. (1997) 10:165–70.
14. Vincent JL, Patel GH, Fox MD, Snyder AZ, Baker JT, Van Essen DC, et al. Intrinsic functional architecture in the anaesthetized monkey brain. *Nature*. (2007) 447:83–6. doi: 10.1038/nature05758
15. Smith SM, Fox PT, Miller KL, Glahn DC, Fox PM, Mackay CE, et al. Correspondence of the brain's functional architecture during activation and rest. *Proc Natl Acad Sci USA*. (2009) 106:13040–5. doi: 10.1073/pnas.0905267106
16. Seeley WW, Menon V, Schatzberg AF, Keller J, Glover GH, Kenna H, et al. Dissociable intrinsic connectivity networks for salience processing and executive control. *J Neurosci*. (2007) 27:2349–56. doi: 10.1523/JNEUROSCI.5587-06.2007
17. Raichle ME, Mintun MA. Brain work and brain imaging. *Ann Rev Neurosci*. (2006) 29:449–76. doi: 10.1146/annurev.neuro.29.051605.112819
18. Greicius M. Resting-state functional connectivity in neuropsychiatric disorders. *Curr Opin Neurol*. (2008) 21:424–30. doi: 10.1097/WCO.0b013e328306f2c5
19. Fineberg NA, Potenza MN, Chamberlain SR, Berlin HA, Menzies L, Bechara A, et al. Probing compulsive and impulsive behaviors, from animal models to endophenotypes: a narrative review. *Neuropsychopharmacology*. (2010) 35:591–604. doi: 10.1038/npp.2009.185
20. Feil J, Sheppard D, Fitzgerald PB, Yucel M, Lubman DI, Bradshaw JL. Addiction, compulsive drug seeking, the role of frontostriatal mechanisms in regulating inhibitory control. *Neurosci Biobehav Rev*. (2010) 35:248–75. doi: 10.1016/j.neubiorev.2010.03.001
21. Camchong J, MacDonald AW III, Nelson B, Bell C, Mueller BA, Specker S, et al. Frontal hyperconnectivity related to discounting and reversal learning in cocaine subjects. *Biol Psychiat*. (2011) 69:1117–23. doi: 10.1016/j.biopsych.2011.01.008
22. Sakai Y, Narumoto J, Nishida S, Nakamae T, Yamada K, Nishimura T, et al. Corticostriatal functional connectivity in non-medicated patients with obsessive-compulsive disorder. *Eur Psychiat*. (2011) 26:463–9. doi: 10.1016/j.eurpsy.2010.09.005
23. Wilcox CE, Teshiba TM, Merideth F, Ling J, Mayer AR. Enhanced cue reactivity and fronto-striatal functional connectivity in cocaine use disorders. *Drug Alcohol Depend*. (2011) 115:137–44. doi: 10.1016/j.drugalcdep.2011.01.009
24. Konova AB, Moeller SJ, Goldstein RZ. Common and distinct neural targets of treatment: changing brain function in substance addiction. *Neurosci Biobehav Rev*. (2013) 37:2806–17. doi: 10.1016/j.neubiorev.2013.10.002
25. Koehler S, Ovadia-Caro S, van der Meer E, Villringer A, Heinz A, Romanczuk-Seiferth N, et al. Increased functional connectivity between prefrontal cortex and reward system in pathological gambling. *PLoS ONE*. (2013) 8:e84565. doi: 10.1371/journal.pone.0084565
26. Tomasi D, Volkow ND. Striatocortical pathway dysfunction in addiction and obesity: differences and similarities. *Crit Rev Biochem Mol Biol*. (2013) 48:1–19. doi: 10.3109/10409238.2012.735642
27. Abe Y, Sakai Y, Nishida S, Nakamae T, Yamada K, Fukui K, et al. Hyper-influence of the orbitofrontal cortex over the ventral striatum in obsessive-compulsive disorder. *Eur Neuropsychopharmacol*. (2015) 25:1898–905. doi: 10.1016/j.euroneuro.2015.08.017
28. Wisner KM, Patzelt EH, Lim KO, MacDonald AW III. An intrinsic connectivity network approach to insula-derived dysfunctions among cocaine users. *Am J Drug Alcohol Abuse*. (2013) 39:403–13. doi: 10.3109/00952990.2013.848211
29. Wang W, Wang YR, Qin W, Yuan K, Tian J, Li Q, et al. Changes in functional connectivity of ventral anterior cingulate cortex in heroin abusers. *Chin Med J*. (2010) 123:1582–8. doi: 10.3760/cma.j.issn.0366-6999.2010.12.019
30. Hong LE, Hodgkinson CA, Yang Y, Sampath H, Ross TJ, Buchholz B, et al. A genetically modulated, intrinsic cingulate circuit supports human nicotine addiction. *Proc Natl Acad Sci USA*. (2010) 107:13509–14. doi: 10.1073/pnas.1004745107
31. Hong LE, Gu H, Yang Y, Ross TJ, Salmeron BJ, Buchholz B, et al. Association of nicotine addiction and nicotine's actions with separate cingulate cortex functional circuits. *Arch Gen Psychiatry*. (2009) 66:431–41. doi: 10.1001/archgenpsychiatry.2009.2
32. Lin F, Zhou Y, Du Y, Zhao Z, Qin L, Xu J, et al. Aberrant corticostriatal functional circuits in adolescents with Internet addiction disorder. *Front Hum Neurosci*. (2015) 9:356. doi: 10.3389/fnhum.2015.00356
33. Yuan K, Yu D, Bi Y, Li Y, Guan Y, Liu J, et al. The implication of frontostriatal circuits in young smokers: a resting-state study. *Hum Brain Mapp*. (2016) 37:2013–26. doi: 10.1002/hbm.23153
34. Fontenelle LF, Harrison BJ, Pujol J, Davey CG, Fornito A, Bora E, et al. Brain functional connectivity during induced sadness in patients with obsessive-compulsive disorder. *J Psychiat Neurosci*. (2012) 37:231–40. doi: 10.1503/jpn.110074
35. Ma N, Liu Y, Li N, Wang CX, Zhang H, Jiang XF, et al. Addiction related alteration in resting-state brain connectivity. *NeuroImage*. (2010) 49:738–44. doi: 10.1016/j.neuroimage.2009.08.037
36. Jasinska AJ, Chen BT, Bonci A, Stein EA. Dorsal medial prefrontal cortex (MPFC) circuitry in rodent models of cocaine use: implications for drug addiction therapies. *Add Biol*. (2015) 20:215–26. doi: 10.1111/adb.12132
37. Jasinska AJ, Stein EA, Kaiser J, Naumer MJ, Yalachkov Y. Factors modulating neural reactivity to drug cues in addiction: a survey of human neuroimaging studies. *Neurosci Biobehav Rev*. (2014) 38:1–16. doi: 10.1016/j.neubiorev.2013.10.013
38. Guadagnin V, Parazzini M, Fiocchi S, Liorni I, Ravazzani P. Deep transcranial magnetic stimulation: modeling of different coil configurations. *IEEE Trans Biomed Eng*. (2016) 63:1543–50. doi: 10.1109/TBME.2015.2498646
39. Fiocchi S, Longhi M, Ravazzani P, Roth Y, Zangen A, Parazzini M. Modelling of the electric field distribution in deep transcranial magnetic stimulation in the adolescence, in the adulthood, and in the old age. *Comput Math Methods Med*. (2016) 2016:9039613. doi: 10.1155/2016/9039613
40. Roth Y, Amir A, Levkovitz Y, Zangen A. Three-dimensional distribution of the electric field induced in the brain by transcranial magnetic stimulation using figure-8 and deep H-coils. *J Clin Neurophysiol*. (2007) 24:31–8. doi: 10.1097/WNP.0b013e31802fa393
41. Hadland KA, Rushworth MF, Passingham RE, Jahanshahi M, Rothwell JC. Interference with performance of a response selection task that has no working memory component: an rTMS comparison of the dorsolateral prefrontal and medial frontal cortex. *J Cogn Neurosci*. (2001) 13:1097–108. doi: 10.1162/089892901753294392

42. Rushworth MF, Hadland KA, Paus T, Sipila PK. Role of the human medial frontal cortex in task switching: a combined fMRI and TMS study. *J Neurophysiol*. (2002) 87:2577–92. doi: 10.1152/jn.2002.87.5.2577
43. Levkovitz Y, Roth Y, Harel EV, Braw Y, Sheer A, Zangen A. A randomized controlled feasibility and safety study of deep transcranial magnetic stimulation. *Clin Neurophysiol*. (2007) 118:2730–44. doi: 10.1016/j.clinph.2007.09.061
44. Rossi S, Hallett M, Rossini PM, Pascual-Leone A, Safety of TMS Consensus Group. Safety of, Safety, ethical considerations, and application guidelines for the use of transcranial magnetic stimulation in clinical practice and research. *Clin Neurophysiol*. (2009) 120:2008–39. doi: 10.1016/j.clinph.2009.08.016
45. Kundu P, Brenowitz ND, Voon V, Worbe Y, Vertes PE, Inati SJ, et al. Integrated strategy for improving functional connectivity mapping using multiecho fMRI. *Proc Natl Acad Sci USA*. (2013) 110:16187–92. doi: 10.1073/pnas.1301725110
46. Kundu P, Inati SJ, Evans JW, Luh WM, Bandettini PA. Differentiating BOLD and non-BOLD signals in fMRI time series using multi-echo EPI. *NeuroImage*. (2012) 60:1759–70. doi: 10.1016/j.neuroimage.2011.12.028
47. Whitfield-Gabrieli S, Nieto-Castanon A. Conn: a functional connectivity toolbox for correlated and anticorrelated brain networks. *Brain Connect*. (2012) 2:125–41. doi: 10.1089/brain.2012.0073
48. Brett AJM, Valabregue R, Poline JB. Region of interest analysis using an SPMtoolbox. In: *Presented at the 8th International Conference on Functional Mapping of the Human Brain Available on CD-ROM in NeuroImage*, 2–6 June 2002. Sendai (2002).
49. Murray GK, Corlett PR, Clark L, Pessiglione M, Blackwell AD, Honey G, et al. Substantia nigra/ventral tegmental reward prediction error disruption in psychosis. *Mol Psychiat*. (2008) 239:267–76. doi: 10.1038/sj.mp.4002058
50. Martinez D, Slifstein M, Broft A, Mawlawi O, Hwang DR, Huang Y, et al. Imaging human mesolimbic dopamine transmission with positron emission tomography. Part II: amphetamine-induced dopamine release in the functional subdivisions of the striatum. *J Cereb Blood Flow Metabol*. (2003) 23:285–300. doi: 10.1097/01.WCB.0000048520.34839.1A
51. Rosazza C, Minati L, Ghielmetti F, Mandelli ML, Bruzzone MG. Functional connectivity during resting-state functional MR imaging: study of the correspondence between independent component analysis and region-of-interest-based methods. *AJNR*. (2012) 33:180–7. doi: 10.3174/ajnr.A2733
52. Beckmann CF, Smith SM. Probabilistic independent component analysis for functional magnetic resonance imaging. *IEEE Trans Med Imaging*. (2004) 23:137–52. doi: 10.1109/TMI.2003.822821
53. Kiviniemi V, Kantola JH, Jauhiainen J, Hyvarinen A, Tervonen O. Independent component analysis of nondeterministic fMRI signal sources. *NeuroImage*. (2003) 19:253–60. doi: 10.1016/S1053-8119(03)00097-1
54. Zuo XN, Kelly C, Adelstein JS, Klein DF, Castellanos FX, Milham MP. Reliable intrinsic connectivity networks: test-retest evaluation using ICA and dual regression approach. *NeuroImage*. (2010) 49:2163–77. doi: 10.1016/j.neuroimage.2009.10.080
55. Nichols TE, Holmes AP. Nonparametric permutation tests for functional neuroimaging: a primer with examples. *Hum Brain Mapp*. (2002) 15:1–25. doi: 10.1002/hbm.1058
56. Obeso I, Cho SS, Antonelli F, Houle S, Jahanshahi M, Ko JH, et al. Stimulation of the pre-SMA influences cerebral blood flow in frontal areas involved with inhibitory control of action. *Brain Stimulat*. (2013) 6:769–76. doi: 10.1016/j.brs.2013.02.002
57. Fox MD, Buckner RL, White MP, Greicius MD, Pascual-Leone A. Efficacy of transcranial magnetic stimulation targets for depression is related to intrinsic functional connectivity with the subgenual cingulate. *Biol Psychiat*. (2012) 72:595–603. doi: 10.1016/j.biopsych.2012.04.028
58. Nordenskjold A, Martensson B, Pettersson A, Heintz E, Landen M. Effects of Hesel-coil deep transcranial magnetic stimulation for depression - a systematic review. *Nordic J Psychiat*. (2016) 70: 492–7. doi: 10.3109/08039488.2016.1166263
59. Kedzior KK, Gierke L, Gellersen HM, Berlim MT. Cognitive functioning and deep transcranial magnetic stimulation (DTMS) in major psychiatric disorders: a systematic review. *J Psychiat Res*. (2016) 75:107–15. doi: 10.1016/j.jpsychires.2015.12.019
60. Ceccanti M, Inghilleri M, Attilia ML, Raccah R, Fiore M, Zangen A, et al. Deep TMS on alcoholics: effects on cortisolemia and dopamine pathway modulation. A pilot study. *Can J Physiol Pharmacol*. (2015) 93:283–90. doi: 10.1139/cjpp-2014-0188
61. Dinur-Klein L, Dannon P, Hadar A, Rosenberg O, Roth Y, Kotler M, et al. Smoking cessation induced by deep repetitive transcranial magnetic stimulation of the prefrontal and insular cortices: a prospective, randomized controlled trial. *Biol Psychiat*. (2014) 76:742–9. doi: 10.1016/j.biopsych.2014.05.020
62. Spagnolo F, Volonte MA, Fichera M, Chieffo R, Houdayer E, Bianco M, et al. Excitatory deep repetitive transcranial magnetic stimulation with H-coil as add-on treatment of motor symptoms in Parkinson's disease: an open label, pilot study. *Brain Stimul*. (2014) 7:297–300. doi: 10.1016/j.brs.2013.10.007
63. Kranz G, Shamim EA, Lin PT, Kranz GS, Hallett M. Transcranial magnetic brain stimulation modulates blepharospasm: a randomized controlled study. *Neurology*. (2010) 75:1465–71. doi: 10.1212/WNL.0b013e3181f8814d
64. Rapinesi C, Del Casale A, Scatena P, Kotzalidis GD, Di Pietro S, Ferri VR, et al. Add-on deep Transcranial Magnetic Stimulation (dTMS) for the treatment of chronic migraine: a preliminary study. *Neurosci Lett*. (2016) 623:7–12. doi: 10.1016/j.neulet.2016.04.058
65. Tofts PS. The distribution of induced currents in magnetic stimulation of the nervous system. *Phys Med Biol*. (1990) 35:1119–28. doi: 10.1088/0031-9155/35/8/008
66. Stokes MG, Chambers CD, Gould IC, Henderson TR, Janko NE, Allen NB, et al. Simple metric for scaling motor threshold based on scalp-cortex distance: application to studies using transcranial magnetic stimulation. *J Neurophysiol*. (2005) 94:4520–7. doi: 10.1152/jn.00067.2005
67. Trillenberg P, Bremer S, Oung S, Erdmann C, Schweikard A, Richter L. Variation of stimulation intensity in transcranial magnetic stimulation with depth. *J Neurosci Methods*. (2012) 211:185–90. doi: 10.1016/j.jneumeth.2012.09.007
68. Brasil-Neto JP, Cohen LG, Panizza M, Nilsson J, Roth BJ, Hallett M. Optimal focal transcranial magnetic activation of the human motor cortex: effects of coil orientation, shape of the induced current pulse, and stimulus intensity. *J Clin Neurophysiol*. (1992) 9:132–6. doi: 10.1097/00004691-199201000-00014
69. Fox PT, Narayana S, Tandon N, Sandoval H, Fox SP, Kochunov P, et al. Column-based model of electric field excitation of cerebral cortex. *Hum Brain Mapp*. (2004) 22:1–14. doi: 10.1002/hbm.20006
70. Balslev D, Braet W, McAllister C, Miall RC. Inter-individual variability in optimal current direction for transcranial magnetic stimulation of the motor cortex. *J Neurosci Methods*. (2007) 162:309–13. doi: 10.1016/j.jneumeth.2007.01.021
71. Opitz A, Windhoff M, Heidemann RM, Turner R, Thielscher A. How the brain tissue shapes the electric field induced by transcranial magnetic stimulation. *NeuroImage*. (2011) 58:849–59. doi: 10.1016/j.neuroimage.2011.06.069
72. Thielscher A, Opitz A, Windhoff M. Impact of the gyral geometry on the electric field induced by transcranial magnetic stimulation. *NeuroImage*. (2011) 54:234–43. doi: 10.1016/j.neuroimage.2010.07.061
73. Bijsterbosch JD, Barker AT, Lee KH, Woodruff PW. Where does transcranial magnetic stimulation (TMS) stimulate? Modelling of induced field maps for some common cortical and cerebellar targets. *Med Biol Eng Comput*. (2012) 50:671–81. doi: 10.1007/s11517-012-0922-8
74. Janssen AM, Oostendorp TF, Stegeman DF. The coil orientation dependency of the electric field induced by TMS for M1 and other brain areas. *J Neuroeng Rehabil*. (2015) 12:47. doi: 10.1186/s12984-015-0036-2
75. Janssen AM, Rampersad SM, Lucka F, Lanfer B, Lew S, Aydin U, et al. The influence of sulcus width on simulated electric fields induced by transcranial magnetic stimulation. *Phys Med Biol*. (2013) 58:4881–96. doi: 10.1088/0031-9155/58/14/4881
76. Janssen AM, Oostendorp TF, Stegeman DF. The effect of local anatomy on the electric field induced by TMS: evaluation at 14 different target sites. *Med Biol Eng Comput*. (2014) 52:873–83. doi: 10.1007/s11517-014-1190-6
77. Lu M, Ueno S. Calculating the induced electromagnetic fields in real human head by deep transcranial magnetic stimulation. In: *35th Annual*

International Conference of the IEEE Engineering in Medicine and Biology Society (EMBC 2013), 3–7 July 2013. Osaka (2013). p. 795–8.
78. Deng ZD, Lisanby SH, Peterchev AV. Coil design considerations for deep transcranial magnetic stimulation. *Clin Neurophysiol*. (2014) 125:1202–12. doi: 10.1016/j.clinph.2013.11.038
79. Deng ZD, Lisanby SH, Peterchev AV. Electric field depth-focality tradeoff in transcranial magnetic stimulation: simulation comparison of 50 coil designs. *Brain Stimul*. (2013) 6:1–13. doi: 10.1016/j.brs.2012.02.005
80. Kammer T, Beck S, Erb M, Grodd W. The influence of current direction on phosphene thresholds evoked by transcranial magnetic stimulation. *Clin Neurophysiol*. (2001) 112:2015–21. doi: 10.1016/S1388-2457(01)00673-3
81. Bestmann S, Baudewig J, Siebner HR, Rothwell JC, Frahm J. BOLD MRI responses to repetitive TMS over human dorsal premotor cortex. *NeuroImage*. (2005) 28:22–9. doi: 10.1016/j.neuroimage.2005.05.027
82. Bestmann S, Baudewig J, Siebner HR, Rothwell JC, Frahm J. Functional MRI of the immediate impact of transcranial magnetic stimulation on cortical and subcortical motor circuits. *Eur J Neurosci*. (2004) 19:1950–62. doi: 10.1111/j.1460-9568.2004.03277.x
83. Bestmann S, Ruff CC, Blankenburg F, Weiskopf N, Driver J, Rothwell JC. Mapping causal interregional influences with concurrent TMS-fMRI. *Exp Brain Res*. (2008) 191:383–402. doi: 10.1007/s00221-008-1601-8
84. Strafella AP, Ko JH, Grant J, Fraraccio M, Monchi O. Corticostriatal functional interactions in Parkinson's disease: a rTMS/[11C]raclopride PET study. *Eur J Neurosci*. (2005) 22:2946–52. doi: 10.1111/j.1460-9568.2005.04476.x
85. Sack AT, Kohler A, Linden DE, Goebel R, Muckli L. The temporal characteristics of motion processing in hMT/V5+: combining fMRI and neuronavigated TMS. *NeuroImage*. (2006) 29:1326–35. doi: 10.1016/j.neuroimage.2005.08.027
86. Siebner HR, Bergmann TO, Bestmann S, Massimini M, Johansen-Berg H, Mochizuki H, et al. Consensus paper: combining transcranial stimulation with neuroimaging. *Brain Stimul*. (2009) 2:58–80. doi: 10.1016/j.brs.2008.11.002
87. Speer AM, Benson BE, Kimbrell TK, Wassermann EM, Willis MW, Herscovitch P, et al. Opposite effects of high and low frequency rTMS on mood in depressed patients: relationship to baseline cerebral activity on PET. *J Aff Disord*. (2009) 115:386–94. doi: 10.1016/j.jad.2008.10.006
88. Sibon I, Strafella AP, Gravel P, Ko JH, Booij L, Soucy JP, et al. Acute prefrontal cortex TMS in healthy volunteers: effects on brain 11C-alphaMtrp trapping. *NeuroImage*. (2007) 34:1658–64. doi: 10.1016/j.neuroimage.2006.08.059
89. Ko JH, Monchi O, Ptito A, Bloomfield P, Houle S, Strafella AP. Theta burst stimulation-induced inhibition of dorsolateral prefrontal cortex reveals hemispheric asymmetry in striatal dopamine release during a set-shifting task: a TMS-[(11)C]raclopride PET study. *Eur J Neurosci*. (2008) 28:2147–55. doi: 10.1111/j.1460-9568.2008.06501.x
90. Speer AM, Kimbrell TA, Wassermann EM, Willis MW, Herscovitch P, Post RM. Opposite effects of high and low frequency rTMS on regional brain activity in depressed patients. *Biol Psychiat*. (2000) 48:1133–41. doi: 10.1016/S0006-3223(00)01065-9
91. Chen R, Classen J, Gerloff C, Celnik P, Wassermann EM, Hallett M, et al. Depression of motor cortex excitability by low-frequency transcranial magnetic stimulation. *Neurology*. (1997) 48:1398–403. doi: 10.1212/WNL.48.5.1398
92. Wassermann EM, Grafman J, Berry C, Hollnagel C, Wild K, Clark K, et al. Use and safety of a new repetitive transcranial magnetic stimulator. *Electroencephalogra Clin Neurophysiol*. (1996) 101:412–7. doi: 10.1016/0924-980X(96)96004-X
93. Gerschlager W, Siebner HR, Rothwell JC. Decreased corticospinal excitability after subthreshold 1 Hz rTMS over lateral premotor cortex. *Neurology*. (2001) 57:449–55. doi: 10.1212/WNL.57.3.449
94. Strens LH, Oliviero A, Bloem BR, Gerschlager W, Rothwell JC, Brown P. The effects of subthreshold 1 Hz repetitive TMS on cortico-cortical and interhemispheric coherence. *Clin Neurophysiol*. (2002) 113:1279–85. doi: 10.1016/S1388-2457(02)00151-7
95. Rubia K. Functional brain imaging across development. *Eur Child Adolesc Psychiat*. (2013) 22:719–31. doi: 10.1007/s00787-012-0291-8
96. Provost JS, Hanganu A, Monchi O. Neuroimaging studies of the striatum in cognition Part I: healthy individuals. *Front Syst Neurosci*. (2015) 9:140. doi: 10.3389/fnsys.2015.00140
97. Bush G, Luu P, Posner MI. Cognitive and emotional influences in anterior cingulate cortex. *Trends Cogn Sci*. (2000) 4:215–222. doi: 10.1016/S1364-6613(00)01483-2
98. Botvinick MM, Cohen JD, Carter CS. Conflict monitoring and anterior cingulate cortex: an update. *Trends Cogn Sci*. (2004) 8:539–46. doi: 10.1016/j.tics.2004.10.003
99. Li CS, Sinha R. Inhibitory control and emotional stress regulation: neuroimaging evidence for frontal-limbic dysfunction in psycho-stimulant addiction. *Neurosci Biobehav Rev*. (2008) 32:581–97. doi: 10.1016/j.neubiorev.2007.10.003
100. Chambers CD, Garavan H, Bellgrove MA. Insights into the neural basis of response inhibition from cognitive and clinical neuroscience. *Neurosci Biobehav Rev*. (2009) 33:631–46. doi: 10.1016/j.neubiorev.2008.08.016
101. Schultz W, Dayan P, Montague PR. A neural substrate of prediction and reward. *Science*. (1997) 275:1593–9. doi: 10.1126/science.275.5306.1593
102. Corbit LH, Muir JL, Balleine BW. The role of the nucleus accumbens in instrumental conditioning: Evidence of a functional dissociation between accumbens core and shell. *J Neurosci*. (2001) 21:3251–60. doi: 10.1523/JNEUROSCI.21-09-03251.2001
103. Pessiglione M, Seymour B, Flandin G, Dolan RJ, Frith CD. Dopamine-dependent prediction errors underpin reward-seeking behaviour in humans. *Nature*. (2006) 442:1042–5. doi: 10.1038/nature05051
104. Harrison BJ, Soriano-Mas C, Pujol J, Ortiz H, Lopez-Sola M, Hernandez-Ribas R, et al. Altered corticostriatal functional connectivity in obsessive-compulsive disorder. *Arch Gen Psychiat*. (2009) 66:1189–200. doi: 10.1001/archgenpsychiatry.2009.152
105. Cocchi L, Harrison BJ, Pujol J, Harding IH, Fornito A, Pantelis C, et al. Functional alterations of large-scale brain networks related to cognitive control in obsessive-compulsive disorder. *Hum Brain Mapp*. (2012) 33:1089–106. doi: 10.1002/hbm.21270
106. Anticevic A, Hu S, Zhang S, Savic A, Billingslea E, Wasylink S, et al. Global resting-state functional magnetic resonance imaging analysis identifies frontal cortex, striatal, and cerebellar dysconnectivity in obsessive-compulsive disorder. *Biol Psychiat*. (2014) 75:595–605. doi: 10.1016/j.biopsych.2013.10.021
107. Goldstein RZ, Volkow ND. Dysfunction of the prefrontal cortex in addiction: neuroimaging findings and clinical implications. *Nat Rev Neurosci*. (2011) 12:652–69. doi: 10.1038/nrn3119
108. Kuhn S, Gallinat J. Common biology of craving across legal and illegal drugs - a quantitative meta-analysis of cue-reactivity brain response. *Eur J Neurosci*. (2011) 33:1318–26. doi: 10.1111/j.1460-9568.2010.07590.x
109. Abelson JL, Curtis GC, Sagher O, Albucher RC, Harrigan M, Taylor SF, et al. Deep brain stimulation for refractory obsessive-compulsive disorder. *Biol Psychiat*. (2005) 57:510–6. doi: 10.1016/j.biopsych.2004.11.042
110. Mallet L, Polosan M, Jaafari N, Baup N, Welter ML, Fontaine D, et al. Subthalamic nucleus stimulation in severe obsessive-compulsive disorder. *N Engl J Med*. (2008) 359:2121–34. doi: 10.1056/NEJMoa0708514
111. Figee M, Luigjes J, Smolders R, Valencia-Alfonso CE, van Wingen G, de Kwaasteniet B, et al. Deep brain stimulation restores frontostriatal network activity in obsessive-compulsive disorder. *Nat Neurosci*. (2013) 16:386–7. doi: 10.1038/nn.3344
112. O'Reardon JP, Solvason HB, Janicak PG, Sampson S, Isenberg KE, Nahas Z, et al. Efficacy and safety of transcranial magnetic stimulation in the acute treatment of major depression: a multisite randomized controlled trial. *Biol Psychiatry*. (2007) 62:1208–16. doi: 10.1016/j.biopsych.2007.01.018
113. Sachdev PS, Loo CK, Mitchell PB, McFarquhar TF, Malhi GS. Repetitive transcranial magnetic stimulation for the treatment of obsessive compulsive disorder: a double-blind controlled investigation. *Psychol Med*. (2007) 37:1645–9. doi: 10.1017/S0033291707001092
114. Dunlop K, Woodside B, Olmsted M, Colton P, Giacobbe P, Downar J. Reductions in cortico-striatal hyperconnectivity accompany successful treatment of obsessive-compulsive disorder with dorsomedial prefrontal rTMS. *Neuropsychopharmacology*. (2016) 41:1395–403. doi: 10.1038/npp.2015.292
115. Mantovani A, Lisanby SH, Pieraccini F, Ulivelli M, Castrogiovanni P, Rossi S. Repetitive transcranial magnetic stimulation (rTMS) in the treatment of obsessive-compulsive disorder (OCD) and Tourette's syndrome (TS*). Int J Neuropsychopharmacol*. (2006) 9:95–100. doi: 10.1017/S1461145705005729
116. Mantovani A, Simpson HB, Fallon BA, Rossi S, Lisanby SH. Randomized sham-controlled trial of repetitive transcranial magnetic

stimulation in treatment-resistant obsessive-compulsive disorder. *Int J Neuropsychopharmacol*. (2010) 13:217–27. doi: 10.1017/S1461145709990435

117. Bloch Y, Arad S, Levkovitz Y. Deep TMS add-on treatment for intractable Tourette syndrome: a feasibility study. *World J Biol Psychiat*. (2014)17:557–61. doi: 10.3109/15622975.2014.964767
118. Ziemann U. TMS induced plasticity in human cortex. *Rev Neurosci*. (2004) 15:253–66. doi: 10.1515/REVNEURO.2004.15.4.253
119. Di Lazzaro V, Pilato F, Dileone M, Profice P, Oliviero A, Mazzone P, et al. Low-frequency repetitive transcranial magnetic stimulation suppresses specific excitatory circuits in the human motor cortex. *J Physiol*. (2008) 586:4481–7. doi: 10.1113/jphysiol.2008.159558
120. Popa T, Morris LS, Hunt R, Deng Z, Horovitz S, Mente K, et al. Modulation of resting connectivity between the mesial frontal cortex and basal ganglia. *bioRxiv*. (2018). doi: 10.1101/432609

Conflict of Interest Statement: VV is a Medical Research Council Senior Clinical Fellow (MR/P008747/1). MH may accrue revenue on US Patent #7,407,478 (Issued: August 5, 2008): Coil for Magnetic Stimulation and methods for using the same (H-coil). He has received license fee payments from the NIH (from Brainsway) for licensing of this patent.

The remaining authors declare that the research was conducted in the absence of any commercial or financial relationships that could be construed as a potential conflict of interest.